Single crystalline SnO_2 thin films grown on *m*-plane sapphire substrate by mist chemical vapor deposition

Zenji Yatabe [*,1], Takaaki Tsuda[2], Junya Matsushita[3], Takehide Sato[3], Tatsuya Otabe[2], Koji Sue[3], Shoji Nagaoka[4,6], and Yusui Nakamura[5,6]

[1] Priority Organization for Innovation and Excellence, Kumamoto University, 860-8555 Kumamoto, Japan
[2] Graduate School of Science and Technology, Kumamoto University, 860-8555 Kumamoto, Japan
[3] Faculty of Engineering, Kumamoto University, 860-8555 Kumamoto, Japan
[4] Kumamoto Industrial Research Institute, 862-0901 Kumamoto, Japan
[5] Faculty of Advanced Science and Technology, Kumamoto University, 860-8555 Kumamoto, Japan
[6] Kumamoto Institute for Photo-Electro Organics, 860-0901 Kumamoto, Japan

Received ZZZ, revised ZZZ, accepted ZZZ
Published online ZZZ (Dates will be provided by the publisher.)

Keywords SnO_2, *m*-plane sapphire substrate, mist–CVD, single crystal, .

Tin dioxide (SnO_2) thin films, as a candidate for realizing next-generation electrical and optical devices, were grown on 2-inch diameter *m*-plane sapphire substrates by mist chemical vapour deposition at atmospheric pressure. The SnO_2 thin films were characterized by scanning electron microscope (SEM), atomic force microscope (AFM), X-ray diffraction (XRD) in θ–2θ and ϕ scanning modes, and electron backscatter diffraction (EBSD). Although the SEM and AFM images showed a relatively rough surface morphology, it was found from the XRD and EBSD measurements that SnO_2 films were epitaxially grown on the substrates under optimised growth condition. Epitaxial growth of SnO_2 thin film growth at three typical areas on the substrate was confirmed by the EBSD measurements. It is likely that the single crystalline SnO_2 (001) thin film was formed across the 2-inch sapphire substrate. Finally, the second SnO_2 layer was overgrown on the above single crystalline SnO_2 thin film, which functioned as a buffer layer. This method which drastically improved surface roughness of the second SnO_2 layer.

1 Introduction Oxide semiconductors have recently attracted much attention due to their potential use in the next-generation electronics devices such as thin-film transistor [1], light-emitting diodes [2], solar cells [3], power devices [4] and so on. Tin dioxide (SnO_2) is a direct forbidden band gap [5] oxide semiconductor with unique intrinsic material properties, which include wide band gap (~ 4 eV) [6-10], high exciton binding energy (~ 130 meV) and high carrier mobility (~ 250 $cm^2V^{-1}s^{-1}$) at room temperature [11]. In addition, SnO_2 is a relatively low-cost material because it does not contain minor metals such as gallium. In order to obtain high crystallographic properties of SnO_2, the growth of single crystalline SnO_2 require relatively expensive film formation methods such as metal-organic chemical vapour deposition (MOCVD) [10] or molecular beam epitaxy (MBE) [12,13], which needs vacuum equipment. One alternative approach is a mist chemical vapour deposition (mist-CVD), which can form various oxide semiconductors under atmospheric pressure with a simple and less expensive technique [9,14-19].

Most of the previous studies targeted SnO_2 film grown on *c*-plane and *r*-plane sapphire substrate even under vacuum condition (MOCVD, MBE and so on) and only few studies have focused on the film grown on other planes of sapphire [10]. It is clear that lattice constants of sapphire substrate and SnO_2 film should match as close as possible for hetero-epitaxial deposition to be successful. Since the lattice mismatch (9.5 %) between SnO_2 and the *m*-plane

* Corresponding author: e-mail yatabe@cs.kumamoto-u.ac.jp, Phone: +81 96 342 3845, Fax: +81 96 342 3630

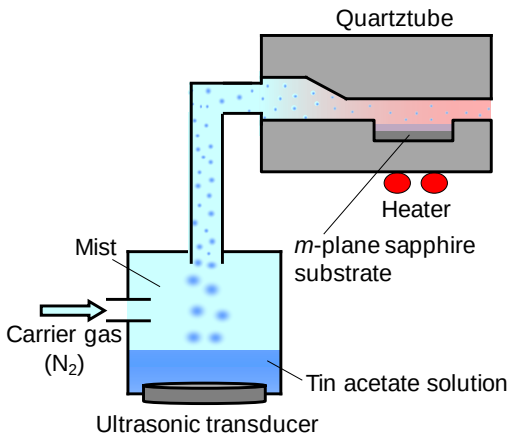

Figure 1 Schematic illustration of the fine-channel type mist-CVD system used in this study.

sapphire along SnO_2 [010] is smaller than that between SnO_2 and *c*-plane (16.0 %), SnO_2 and *r*-plane sapphire (11.3 %) [20], SnO_2 film is favorable to grow on *m*-plane sapphire substrate.

In the present work, SnO_2 films grown on *m*-plane sapphire substrates by mist-CVD involve both low-cost materials and procedures, because Sn and O are abundant, and mist-CVD is a simple atmospheric-pressure process. The detailed structural properties of the films were investigated.

2 Experiments In this study, SnO_2 films were grown using a homemade fine-channel-type mist-CVD system, which was operated at atmospheric pressure. Figure 1 shows a schematic illustration of the mist-CVD system used in this study. The source of the mist was tin(II) acetate ($(CH_3COO)_2Sn$) solution with concentration of 0.04 mol/L. The source solution was ultrasonically atomized at the frequency of 2.4 MHz, and the mist particles were transferred to the reaction area with nitrogen carrier gas with a flow rate of 4 L/min. SnO_2 films were grown on 2-inch diameter *m*-plane sapphire substrates at 525 ºC for 40 min without using any buffer layer. To estimate the thickness of the SnO_2 film, we performed X-ray fluorescence (XRF) measurement at three positions on the sample. The thicknesses of SnO_2 film at three positions on the sample were estimated to be 121, 108 and 114 nm, respectively. Their deviation was 6% from the average (114 nm).

3 Results and discussion We initially performed scanning electron microscope (SEM) and atomic force microscope (AFM) observation to characterize the SnO_2 surface morphology. A top view SEM and AFM images of the SnO_2 surface are shown in Fig. 2. The AFM observation confirmed that the root mean square (RMS) value of a 5×5 μm^2 region is 29 nm. Although the SEM and AFM images showed a relative rough surface morphology as shown Fig.

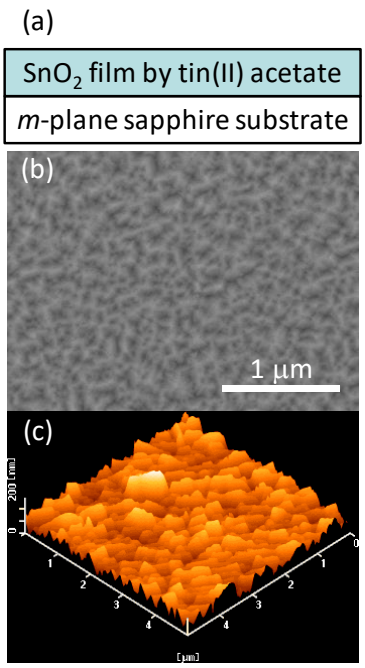

Figure 2 (a) Schematic illustration of the sample structure, (b) top view SEM and (c) AFM images of the SnO_2 film grown by mist-CVD with tin(II) acetate solution.

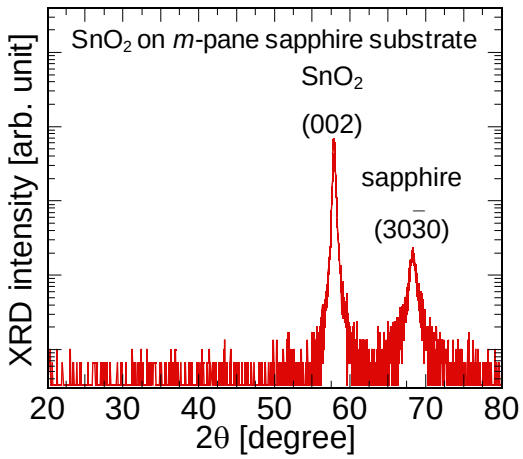

Figure 3 Result of XRD θ-2θ scan for the SnO_2 film grown on *m*-plane sapphire substrate.

2, the SnO_2 surface morphology was much smoother than that of our previous result using the tin(II) chloride aqueous solution (not shown here). The reason for the obtained relatively flat surface morphology formed tin(II) acetate is not clear yet, though tin(II) chloride ($SnCl_2$) is often used as a source solution to grow SnO_2 by mist-CVD [9,18].

To characterize crystallographic properties of the SnO_2 thin film, we carried out X-ray diffraction (XRD) in θ-2θ and ϕ scanning modes. Figure 3 shows the XRD θ-2θ scan patterns measured using incident Cu $K\alpha_1$ radiation. Only the SnO_2 (002) and the sapphire *m*-plane of $(30\bar{3}0)$

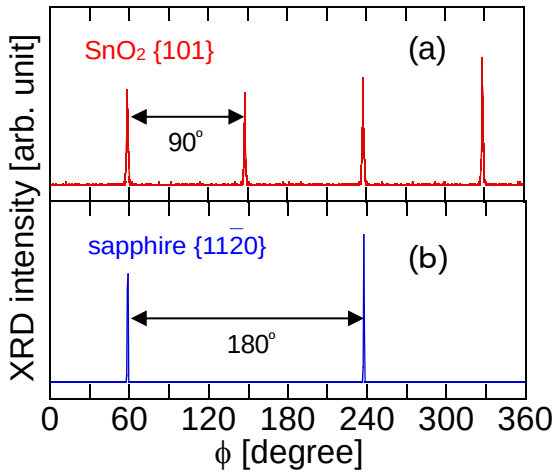

Figure 4 XRD ϕ scan for the (a) SnO_2 film and sapphire substrate.

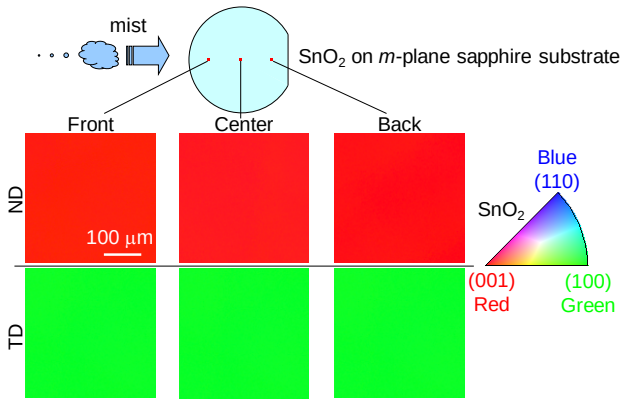

Figure 5 Both normal direction (ND) and transverse direction (TD) of EBSD images at different positions in the SnO_2 film.

were observed in the pattern, indicating that the SnO_2 film was (001) orientated. The XRD ϕ scan was then measured to identify the lateral orientation of the SnO_2 film. The SnO_2 {101} and sapphire {11$\bar{2}$0} planes were used as the monitoring planes. Figure 4 shows the XRD ϕ scan results. Four peaks spaced by 90º were observed for the SnO_2, indicating the fourfold symmetry along [001] axis of SnO_2 with rutile structure and their epitaxial relationship of SnO_2 (001) [100] || sapphire (10$\bar{1}$0) [1$\bar{2}$10] [10]. These θ-2θ and ϕ scan XRD results indicate that the SnO_2 (001) films were epitaxially grown on the sapphire (10$\bar{1}$0) substrates. Note that there was no significant difference among these XRD results at three locations on the sample, which indicate that uniform SnO_2 films were formed. To further investigate the epitaxial growth of the SnO_2 film, electron backscatter diffraction (EBSD) images were analysed to identify the crystallographic orientation at various locations on the sample. The spacing between neighbouring electron beams was 3 μm. Figure 5 shows both normal direction (ND) and transverse direction (TD) of EBSD images of the SnO_2 film.

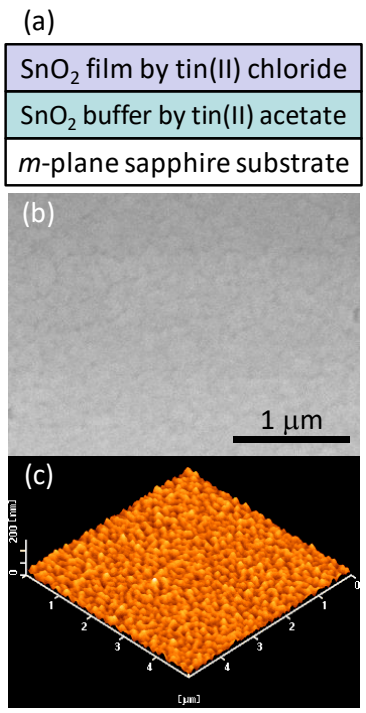

Figure 6 (a) Schematic illustration of the sample structure, (b) top view SEM and (c) AFM images of the SnO_2 film with the buffer layer.

The similarity of the three EBSD images in Fig. 5 indicated that the crystallographic orientation of SnO_2 on the substrate was homogeneous. These results suggest that the single crystalline SnO_2 (001) thin film was formed across the 2-inch diameter *m*-plane (10$\bar{1}$0) sapphire substrate.

Even though the surface was not smooth in the above experiment because no buffer layer was used, surface roughness could be potentially improved using a buffer layer. It is a common knowledge that a hetero-epitaxial semiconductor layers need to be deposited with suitable buffer layers to preserve the high crystalline quality of the over layers [21]. Based on this idea, the single crystalline SnO_2 (001) thin film formed with above condition on the substrate was used as the buffer layer. Second layer of SnO_2 films were overgrown on the single crystalline SnO_2 buffer layer at 800 ºC for 40 min. The source of the mist was changed to tin(II) chloride aqueous solution [9,18] with concentration of 2.5 mol/L. Figure 6 shows a top view SEM and AFM images of the surface of the second SnO_2 layer grown on the buffer layer. The AFM observation confirmed that the RMS value of a 5 × 5 μm^2 region is 9 nm. The SEM and AFM measurements clearly indicated that the surface roughness was drastically improved using the buffer layer, and the detailed characterization will be continued.

4 Conclusion SnO_2 thin films were grown on 2-inch diameter *m*-plane sapphire substrates by mist-CVD at atmospheric pressure. The SnO_2 thin films were characterized by

SEM, XRD and EBSD. It was found from the XRD and EBSD measurements that SnO_2 films were epitaxially grown on the substrates under optimised growth condition. Epitaxial growth of SnO_2 thin film growth at three typical areas on the substrate was confirmed by the EBSD measurements It is likely that the single crystalline SnO_2 (001) thin film was formed across the 2-inch sapphire substrate. Finally, the second SnO_2 layer was overgrown on the above single crystalline SnO_2 thin film, which functioned as a buffer layer. This method which drastically improved surface roughness of the second SnO_2 layer.

Acknowledgements The authors sincerely thank Dr. Tetsuro Sueyoshi of Kumamoto University for his support of the AFM measurements. This work was partly supported by Foundation for Promotion of Material Science and Technology of Japan (MST Foundation).

References

[1] E. Fortunato, P. Barquinha, and R. Martins, Adv. Mater. **24**, 2945 (2012).
[2] Y.-S. Choi, J.-W. Kang, D.-K. Hwang, and S.-Ju Park, IEEE Trans. Electron Dev. **57**, 26 (2010).
[3] S.-C. Lee, J.-H. Lee, T.-S. Oh, Y.-H. Kim, Sol. Energ. Mat. Sol. Cells **75**, 481 (2003).
[4] M. Higashiwaki, K. Sasaki, A. Kuramata, T. Masui, and S. Yamakoshi, Appl. Phys. Lett. **100**, 013504 (2012).
[5] V. T. Agekyan, Phys Stat Solidi A **43**, 11 (1977).
[6] M. Nagasawa, S. Shionoya, and S. Makishima, Jpn. J. Appl. Phys. **4**, 195 (1965).
[7] A. L. Dawar and J. C. Joshi, J. Mater. Sci. **19**, 1 (1984).
[8] R. J. Choundhary, S. B. Ogale, S. R. Shinde, V. N. Kulkarni, T. Venkatesan, K. S. Harshavardhan, M. Strikovski, and B. Hannoyer, Appl. Phys. Lett. **84**, 1483 (2004).
[9] T. Okuno, T. Oshima, S.-D. Lee, and S. Fujita, Phys. Status Solidi C 8, 540 (2011).
[10]Z. Zhu, J. Man, L. Kong, C. Luan, and Q. Yu, J. Cryst. Growth 324, **98** (2011).
[11] J. E. Dominguez, L. Fu, and X. Q. Pan, Appl. Phys. Lett. **81**, 5168 (2002).
[12] M. E. White, M. Y. Tsai, F. Wu, and J. S. Speck, J. Vac. Sci. Technol. A **26**, 1300 (2008).
[13] T. Oshima, T. Okuno, and S. Fujita, Jpn. J. Appl. Phys. **48**, 120207 (2009).
[14] J. G. Lu, T. Kawaharamura, H. Nishinaka, Y. Kamada, T. Ohshima, and S. Fujita, J. Cryst. Growth **299**, 1 (2007).
[15] D. Shinohara and S. Fujita, Jpn. J. Appl. Phys. **47**, 7311 (2008).
[16] J. Piao, S. Katori, T. Kawaharamura, C. Li, and S. Fujita, Jpn. J. Appl. Phys. **51** 090201 (2012).
[17] T. Kawaharamura, T. Uchida, M. Sanada, and M. Furuta, AIP Advances **3**, 032135 (2013).
[18] J.-Y. Bae, J. Park, H. Y. Kim, H.-S. Kim, and J.-S. Park, ACS Appl. Mater. Interfaces **7**, 12074 (2015).
[19] H. Tanoue, T. Taniguchi, S. Wada, S. Yamamoto, S. Nakamura, Y. Naka, H. Yoshikawa, M. Munekata, S. Nagaoka, and Y. Nakamura, Appl. Phys. Express **8**, 125502 (2015).
[20] Y. Lu, Ph.D. thesis, Justus-Liebig-Universität Giessen (2015).
[21] K.-H. Bang, D.-K. Hwang, and J.-M. Myoung, Appl. Surf. Sci. **207**, 359 (2003)